Infiltration capacity based on soil geophysical constants using artificial infiltration in residential land

Totoh Andayono[1,2], Mas Mera[2*], Junaidi[2] and Dalrino[3]

[1] Department of Civil Engineering, Faculty of Engineering, Universitas Negeri Padang, **Indonesia**
[2] Department of Civil Engineering, Faculty of Engineering, Universitas Andalas, **Indonesia**
[3] Department of Civil Engineering, Politeknik Negeri Padang, **Indonesia**

*Corresponding Author: mas_mera@eng.unand.ac.id

Cite this   https://doi.org/10.24036/teknomekanik.v7i2.31372

Abstract: Conversion of catch-land into residential land in urban areas reduces infiltration, and increases surface flow and flood risk. Artificial infiltration is a potential solution to increase infiltration capacity, but its effectiveness is highly dependent on the physical characteristics of the soil, including geophysical constants. This study aims to determine the level of infiltration capacity based on the value of soil geophysical constants using artificial infiltration in residential land in Padang. Measurements were carried out using the Horton method and double-ring infiltrometer in several residential locations. The study results show that the soil characteristics of residential land in Padang consist of the soil texture of sand, loamy sand, and sandy loam, which have high moisture content, large fill weight, and low porosity, causing low infiltration rate and high surface flow. Artificial infiltration can significantly increase the infiltration capacity, especially on sandy soils with high hydraulic conductivity. The soil geophysical constant, k, is classified according to field measurement results. In the lower range of $1.2 < k \leq 1.9$, the average infiltration capacity was found at 625.1 mm/hour. Within the interval of $1.9 < k \leq 2.6$, the mean capacity decreased to 587.7 mm/hour, but in the upper interval of $2.6 < k \leq 3.3$, the average infiltration capacity was 499 mm/hour. Large soil geophysical constants reveal higher infiltration capacity, while small geophysical constants indicate low infiltration capacity.

Keywords: infiltration capacity; artificial infiltration; residential land; geophysical constants

1.   Introduction

Hydrometeorological disasters occupy the top rank of disaster trends in Indonesia, and flood is the most frequent one [1]. Extreme global climate change, weather anomalies, high precipitation, high tides, and human activities cause this trend. Human activity factors such as dumping garbage into rivers, reducing land cover in upstream areas due to illegal logging, and land conversion from catch-land to residential land, especially in urban areas, significantly increase flood intensity [2], [3], [4], [5], [6]. The conversion of catch-land to residential land is a common phenomenon, along with population growth and urbanization in urban areas [7]. These changes lead to a reduced vegetation area and increased soil cover with impermeable materials, so natural infiltration is disrupted. Changes in soil surface conditions can reduce the rate and capacity of infiltration so that there is a reduction in rainwater infiltration, an increase in surface flow, and a reduction in groundwater replenishment. This condition increases the risk of flooding, especially in areas that do not have a good drainage system. Therefore, effective solutions are needed to increase infiltration capacity in urban areas [8], [9], [10], [11].

One of the methods to increase infiltration capacity is artificial infiltration. It is a technique designed to speed up the process of infiltration of water into soil in a certain way [12], [13], [14], [15], [16].

Extensive research has been conducted on the development of artificial infiltration tools. The development of artificial infiltration employs a straightforward design, focusing on management that utilizes natural materials while minimizing the impact on the water cycle. Various artificial infiltration methods are employed to enhance rainwater infiltration in residential land, such as leaky wells, retention trenches, infiltration basins, infiltration cells, seepage pipes, and infiltration galleries [17], [18], [19].

Recent studies discuss the effectiveness of artificial infiltration performance in enhancing the infiltration capacity of infiltration galleries. Infiltration galleries operate on the principle of septic tanks, demonstrating that a 30-meter gallery can decrease runoff by 90%, while a 61-meter gallery can reduce it by up to 85%, with an infiltration rate of 0.64 cm [20]. A different gallery variant employs porous pipes within gravel trenches, demonstrating effectiveness in regions with elevated groundwater levels. This method can decrease surface flow by as much as 60%, depending on soil conditions and pipe design [21]. Furthermore, a distinct type of infiltration gallery was developed that effectively reduced the decline in groundwater levels by 0.15 m/year through the utilization of runoff for aquifer recharge [22]. An infiltration trench, referred to as a sand ditch, is a similar method to a gallery that can enhance infiltration by up to 156% compared to initial conditions and augment drainage volume by a factor of 2.6 [13]. A porous bioretention tank, featuring a gravel layer at the bottom, facilitates water flow through the filter as an alternative artificial infiltration system. The effectiveness of this system depends on the duration of tank drainage, which can mitigate surface runoff volume [23]. The effectiveness of artificial infiltration is strongly influenced by the physical properties of the soil, including soil texture and soil geophysical constants. Therefore, a deep understanding on the characteristics of the soil in a specific location is essential in designing and implementing an effective artificial infiltration system [24], [25], [26].

The value of the geophysical constant has a significant influence on the infiltration capacity of the soil. The geophysical constant (k) in Horton's equation is defined as a coefficient whose value depends on the characteristics of the soil and vegetation cover or is related to the condition of the soil surface. The value k reflects the soil infiltration capacity. The formula k is the value used to describe the initial infiltration rate or the soil's initial capacity to absorb rainwater [27].Variations in the values of these constants can affect how quick and how much water can seep into the soil [28], [29]. The value of k can be calculated by fitting field infiltration experimental data to Horton's equation with a non-linear exponential regression approach.

As one of the cities that continues to develop, Padang faces problems related to water management, especially in reducing the potential of flooding. To design and implement artificial infiltration systems in urban residential land in Padang, a comprehensive understanding on the geophysical constants of the soil is essential. This study aims to determine the geophysical constant of soil in Padang residential land by using artificial infiltration to increase infiltration capacity. Understanding the value of soil geophysical constants in Padang residential land and employing artificial infiltration based on these constants is crucial for fostering sustainable water management strategies. Urban environments seeking to design and implement artificial infiltration systems, aligning with local geophysical conditions and soil textures, is important. This approach hopes to significantly contribute to developing efficient and effective water management practices in these areas [30].

2.   Material and methods

2.1   Research location

The research location is focused on the residential land developed in Padang, West Sumatra, based on the 2010-2030 Regional Spatial Plan of Padang City [26]. The research location is ten residential land in five sub-districts, generally located upstream with a high groundwater level elevation

criterion (> 2 meters) so that artificial infiltration can work properly. Figure 1 presents the results of mapping the location point of the research site.
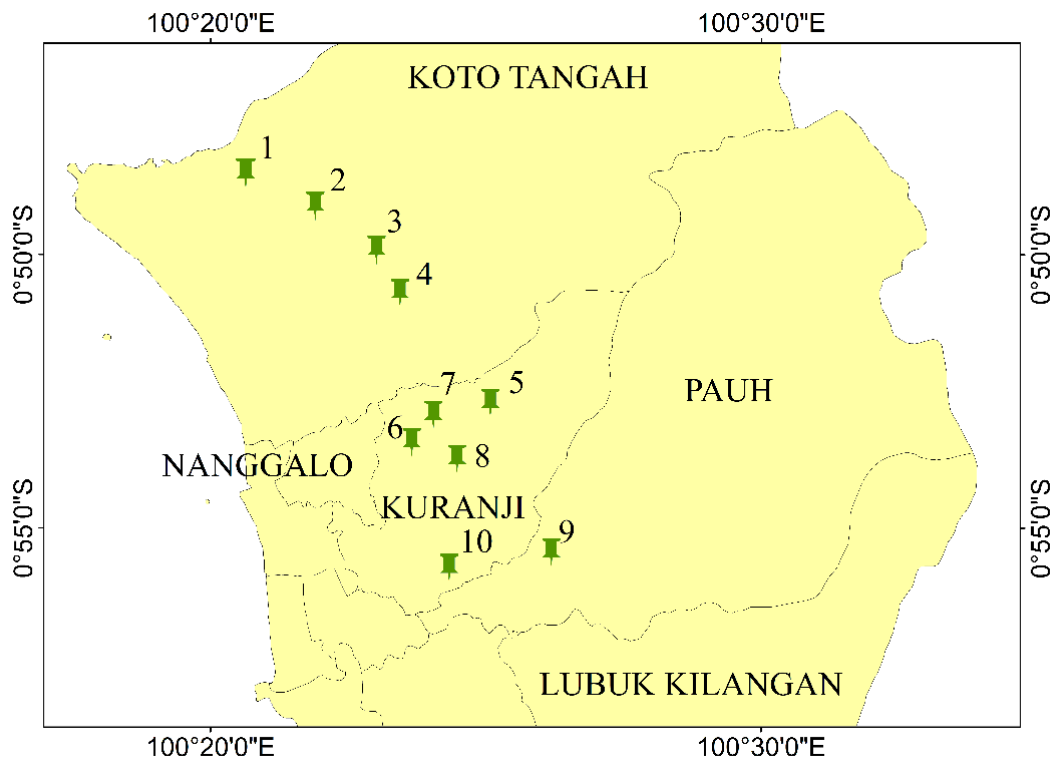

Figure 1.   Research location

2.2   Research stages

This research was carried out in several stages. It began with determining soil characteristics and infiltration in residential land in the research area. Soil parameters were obtained by taking ten residential locations as samples. The sample consisted of disturbed soil samples and undisturbed soil samples. The soil samples were tested to obtain the soil physical characteristics and textures. Infiltration measurements in the soil surface layer used a double-ring infiltrometer three times for one residential land so that 30 infiltration tests were obtained. The infiltration rate was calculated by using Horton's equation as presented in equation 1.

$$f = \frac{\Delta h}{t} \qquad (1)$$

f is the infiltration rate (mm/min), Δh is the height of the drop in a given interval (mm), and t is the time it takes for water at Δh to seep into the soil. The infiltration capacity was calculated based on the results of data processing of the infiltration rate table by using Horton's method. The Horton equation is a mathematical model that describes the rate of soil infiltration as a function of time, as presented in equation 2.

$$f = f_c + (f_o - f_c)e^{-kt} \qquad (2)$$

The value of the constant k in Horton's formula is described by equation 3 and 4.

$$t = \frac{\log(f - f_c)}{-k \log e} - \frac{\log(f_o - f_c)}{-k \log e} \qquad (3)$$

$$t = \left(\frac{1}{-k \log e}\right) \log(f - f_c) + \left(\frac{1}{k \log e}\right) \log(f_o - f_c) \qquad (4)$$

128

f_c is the constant infiltration rate (mm/min), f_o is the initial infiltration rate, e is exponential, and t is the time (minutes). To obtain an unknown parameter of Horton's equation, it must be compared with a linear equation in the form that $y = mx + c$ $y = f$ as shown by equation 5, 6, and 7.

$$m = -\frac{1}{k \log e} \tag{5}$$

$$x = \log(f - f_c) \tag{6}$$

and

$$c = \frac{1}{k \log e} \log(f_o - f_c) \tag{7}$$

Thus, the value of k can be determined by the formula in equation 8.

$$k = -\frac{1}{m \log e} = -\frac{1}{m \log 2{,}718} = -\frac{1}{0{,}434\,m} \tag{8}$$

where m is the gradient obtained from the linear graph of the relationship between time and log $(f - f_c)$.

The second stage was the manufacture and installation of artificial infiltration. Artificial infiltration manufacturing used materials and sizes similar to those of the artificial infiltration tool model. The acrylic material on the model used non-woven geotextile for field testing. Artificial infiltration installations were in the form of excavations (shallow wells) with the same dimensions and equipment as the infiltration model [31].

The third stage was infiltration testing using artificial infiltration. The test was conducted by draining rainwater from the house roof to the house gutter, then flowing through PVC pipes to artificial infiltration. Data collection began when the rain started to fall and lasted when the rain stopped. The parameters measured were the duration of rain t measured with a stopwatch; the height of rain d during time t measured by a rain gauge, which was read every predetermined time interval; the volume of water outflow measured with a measuring cup, and the area of the roof A by measured for the length and width of the roof with water flows to a specific gutter.

The last stage was data analysis, which determined the geophysical constants of soil and its infiltration capacity in Padang residential land using artificial infiltration. The analysis results were the infiltration capacity based on soil texture and soil geophysical constants.

2.3   Testing with and without Artificial Infiltration

Infiltration measurements without artificial infiltration were conducted on the ground surface, utilizing a double ring infiltrometer, with dimensions of 30/55 cm [32], following the implementation technique outlined in Indonesian National Standard (SNI 7752:2012) [33], as seen in Figure 2(a).

The testing by using artificial infiltration refers to infiltration measurement using a double-ring infiltrometer. The volume of incoming water came from rainwater falling from the roof of the house, collected on the house gutters, and flowed through PVC pipes to artificial infiltration during a predetermined Δ time interval t. This volume of water was a puddle of water at the ground level. The rain height d was measured by using a rain gauge during the rain time t measured by utilizing a stopwatch. The volume of inflow water was calculated by multiplying the depth of rain d by the

area of roof A. The outflow volume was measured by collecting water from artificial infiltration by using a measuring cup at an interval equal to the inflow, as seen in Figure 2(b).

Figure 2.   Infiltration test without artificial infiltration and using artificial infiltration

The volume of water seeping into the ground or the volume of infiltration is the volume of incoming water minus the volume of outgoing water. While the height of the water drop Δh is the volume of infiltration divided by the cross-sectional area of the artificial infiltration device A. The instantaneous rate of infiltration ($\Delta h/\Delta t$) is the height of the descent divided by its time interval.

3.   Results and discussion

3.1   Soil characteristics

The soil characteristics in residential land in Padang, which were obtained from the results of measurements and tests, are sand, loamy sand, and sandy loam. The average moisture content ω is 41.9%, the average soil content weight γ is 1.84gr/cm^3, and the average soil specific gravity G_s is 2.66. The groundwater content is in the large category, thus reducing the rate of infiltration. The weight of the soil content is relatively high, indicating that the density is also high. This leads to a denser soil structure and low porosity. This means that there is less pore space in the soil, thus making it difficult for water to seep into the soil, causing small infiltration rate.

The average porosity n is 35.73%, and the density of the soil is solid. The porosity value is in the low category ($n < 35\%$), so it will inhibit infiltration, resulting a small infiltration rate. Solid soils negatively influence infiltration, i.e., reducing the infiltration rate due to low porosity and compact structure. The average soil permeability value of 0.0012 cm/sec for the upper soil layer (< 30cm) and the lower soil layer (>100cm) or under the artificial infiltration installation is 0.0018 cm/sec. The permeability value is classified as very quickly. This condition shows that the soil layer under the landfill can absorb more water compared to the upper layer.

3.2   Infiltration without using artificial infiltration

Infiltration measurements without artificial infiltration used a double-ring infiltrometer. Each location got three infiltration measurement results which were counted for the average rate of each, represented by the curve in Figure 3.
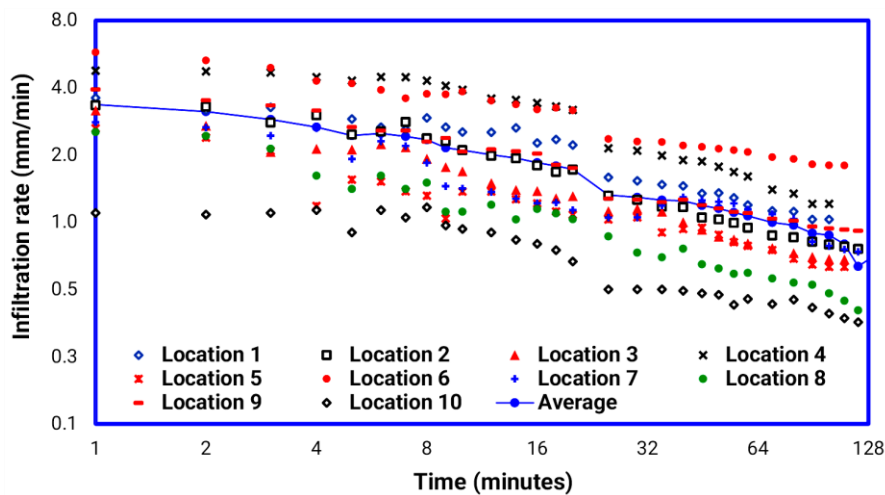
Figure 3.   Infiltration rate without the use of a double-ring infiltrometer

The results of the curve in Figure 3 obtained an average constant infiltration rate (f_c) of 0.85 mm/min or 51.1 mm/hour. Based on the classification of the infiltration area, it is in the very low category (f_c < 0.1 cm/min), while based on the classification, the infiltration rate is in the category of class 3: medium (f_c: 20-63 mm/hour). This condition causes rainwater that falls on the ground surface to take a long time for infiltration so that most of the rainwater will become surface flow. Based on the potential volume of water that can be absorbed, the value of the infiltration rate is only able to permeate a maximum of 150,000 m^3/hour/km^2

The infiltration capacity was calculated using equation 2 based on the results of the infiltration rate measurement, and the initial infiltration rate (f_o) and final infiltration rate were obtained. The value of the geophysical constant, k, was calculated using equation 8. The gradient value, m, was obtained from the linear graph of the time relationship with the log ($f - f_c$). The calculation results for each time interval are presented in the form of an infiltration capacity curve. The infiltration capacity curve for each site and the average of all sites are shown in Figure 4.
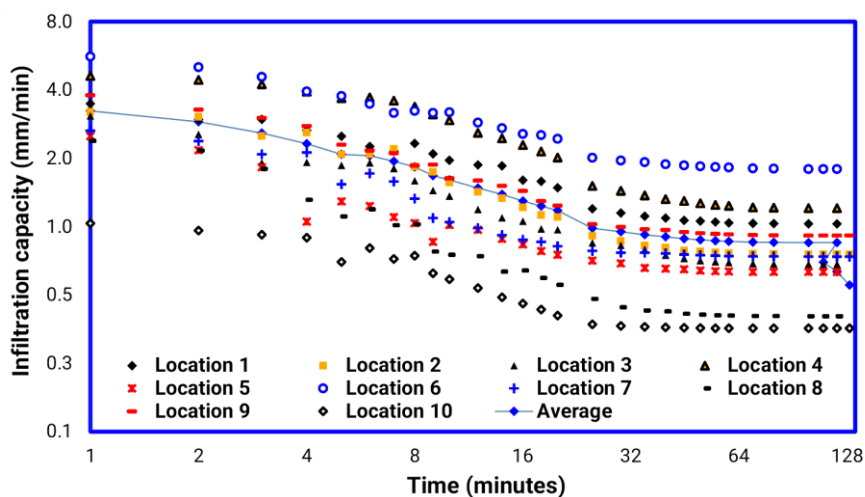

Figure 4.   Infiltration capacity curve without using artificial infiltration

Based on the curve of Figure 4, an average constant infiltration capacity of 0.65 mm/min or 39 mm/hour is obtained. From the curve, it can be seen that the infiltration capacity decreases by time. It can be caused by several factors, ranging from soil density, soil physical properties, and soil porosity.

131

Low infiltration in the top layer of soil in Padang residential land is caused by high soil density, soil properties, soil texture, and fine soil fractions that clog the pores of the soil surface. These factors contribute to producing low infiltration. In contrast, the layer below has a large permeability (permeability k: very fast). To overcome this problem, a method, that is able to funnel water into soil layers where water is hard to seep into a certain depth, is needed. One of the methods is artificial infiltration.

3.3   Infiltration using artificial infiltration

The measurement and infiltration calculation results used artificial infiltration of as many as ten measurements in one location so that for 10 locations, there were 100 measurements. Figure 5(a) is the infiltration rate curve for a single location and Figure 5(b) is the average infiltration rate curve for 10 locations.
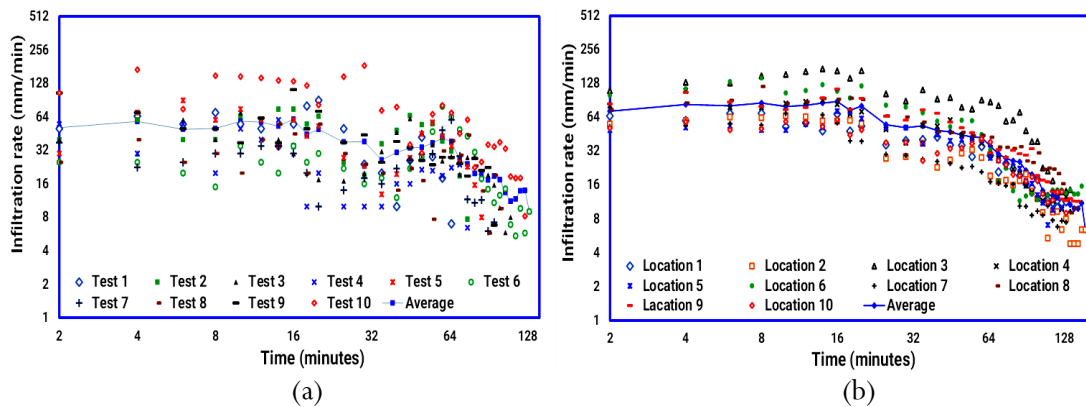

Figure 5.   Infiltration rate using artificial infiltration

The average constant infiltration rate occurs at 130 minutes. From the curve, the average constant infiltration rate (f_c) is obtained for 15.2 mm/min or 912 mm/hour, entering class 7 (very fast). Furthermore, the infiltration capacity curve for ten measurements and one average infiltration capacity curve in one location is shown in Figure 6(a) and the infiltration capacity curve of 10 locations (10 measurements each) averaged arithmetic is shown in Figure 6(b)
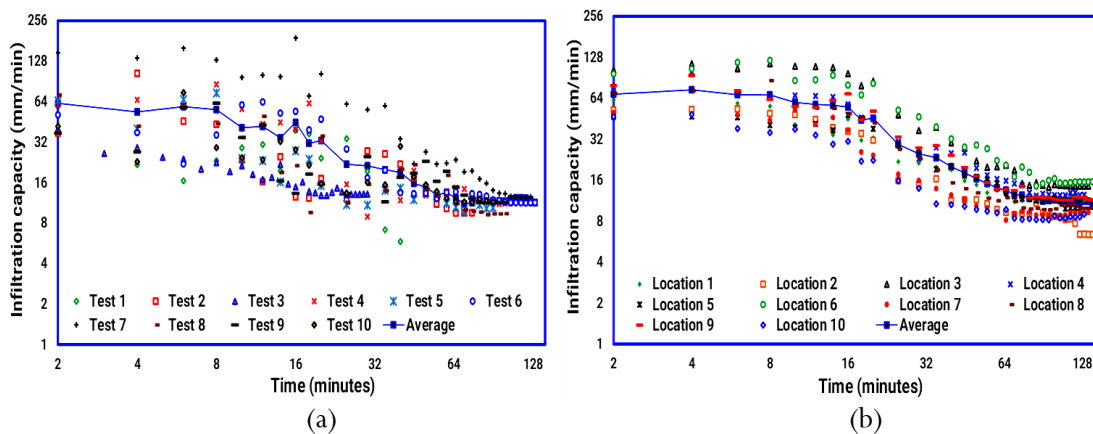

Figure 6.   Infiltration capacity using artificial infiltration

Based on the infiltration capacity curve in residential land using artificial infiltration, an average constant infiltration capacity of 9.55 mm/min or 573 mm/hour was obtained. This means that the use of artificial infiltration in residential land is very effective in increasing the ability of the soil to absorb water from the soil surface.

3.4   Infiltration capacity based on soil texture and geophysical constants

Measurements of infiltration capacity and soil texture were conducted to analyze the relationship between soil texture characteristics and its ability to absorb water as soil texture plays an important role in determining the movement of water in the soil. The test results show three types of soil texture with variations in infiltration capacity, ranging from coarse to fine texture. Figure 7 shows the infiltration capacity curve based on the type of soil texture measured.
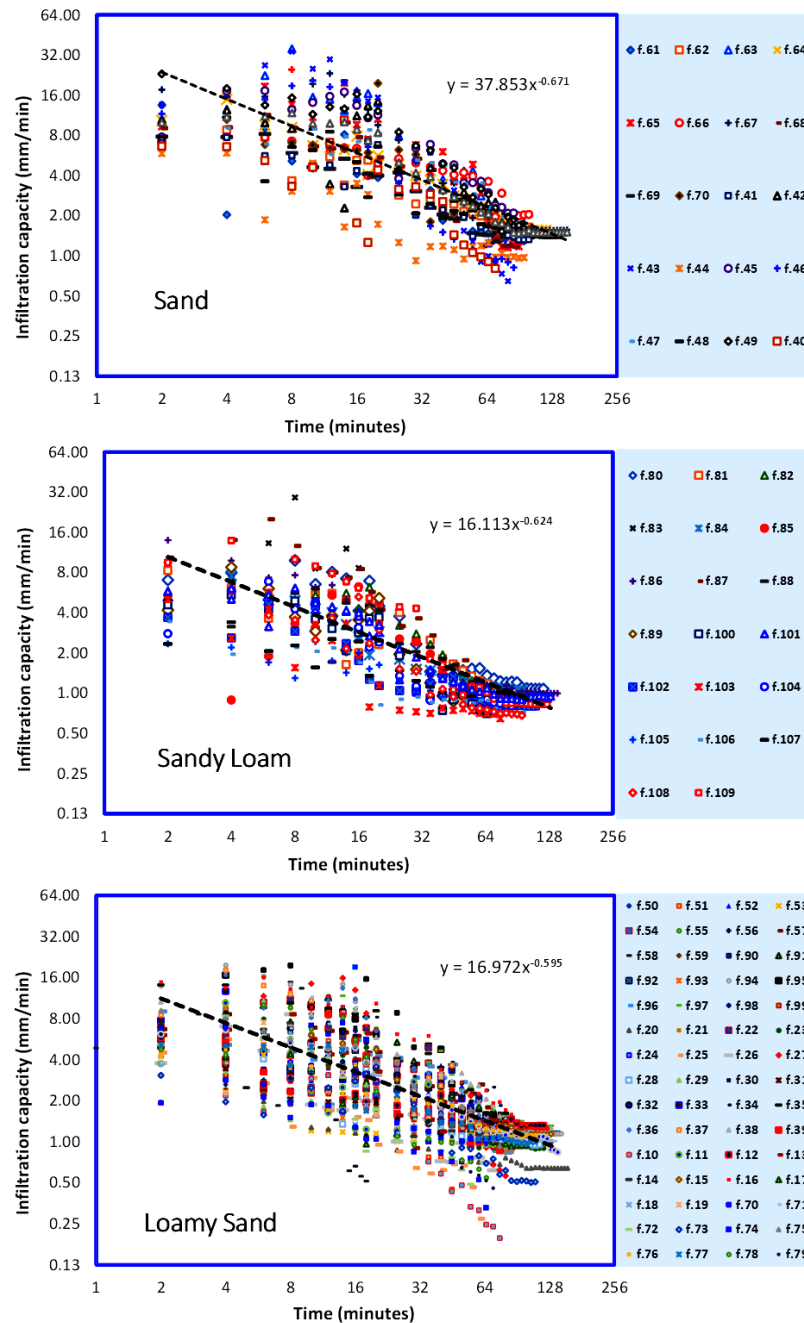

Figure 7.   Infiltration capacity based on soil texture variation

The symbol f on the curve in Figure 8 represents the infiltration capacity determined by equation 2. The estimate is categorized according to identical soil textures derived from 100 infiltration rate tests. The soil texture test findings indicated that 20 samples were classified as sand, 20 as sandy loam, and 60 as loamy sand.

133

The curve analysis results obtained an average infiltration capacity at the loamy sand of 8.96 mm/min or 538.2 mm/hour. The average infiltration capacity of sandy loam soil is 7.73 mm/min or 463.7 mm/hour, and the average infiltration capacity of sand soil is 13.12 mm/min or 787.2 mm/hour. These values show that soil texture significantly influences soil infiltration capacity. Sandy soils have the highest infiltration capacity, with large particles and pore spaces. Water moves faster through sandy soils due to the lack of cohesion between particles, resulting in higher infiltration.

The constant values are divided into three classes, low, medium, and high, to see the influence of the geophysical constant of soil k on the infiltration capacity that occurs based on the measurement results. The following is the infiltration capacity curve shown in Figure 8.
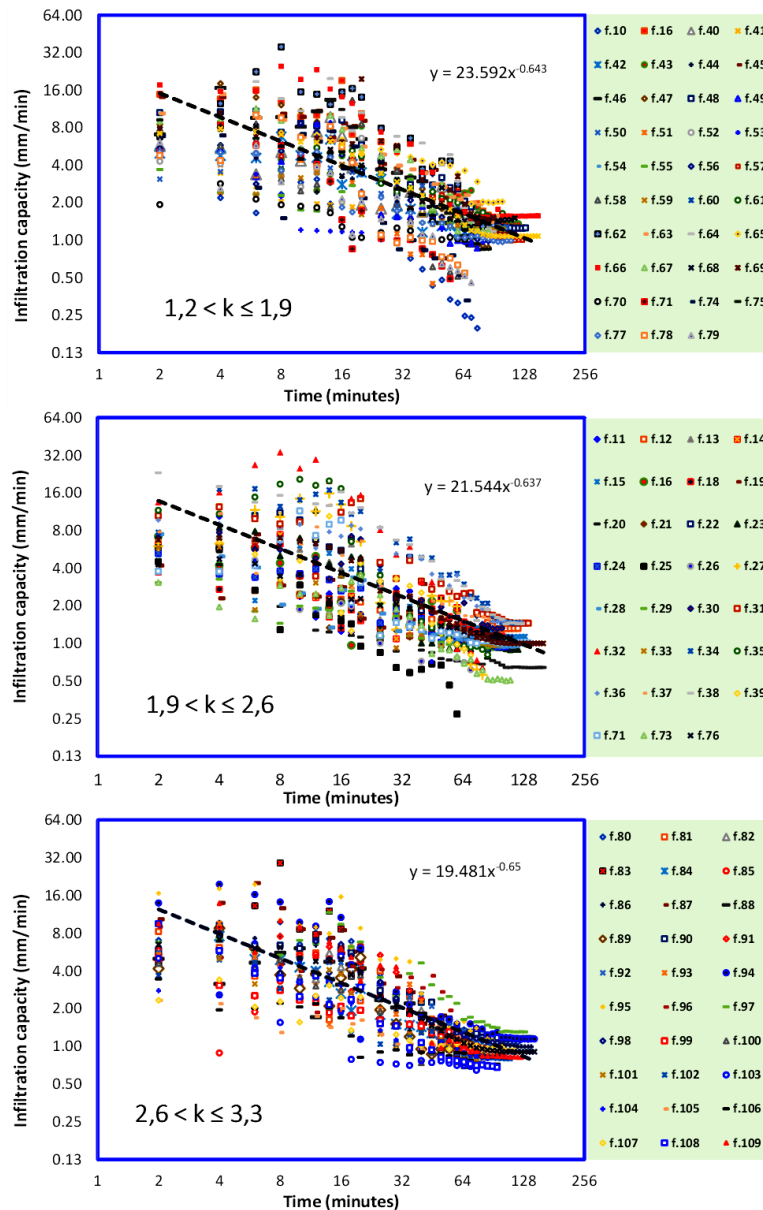

Figure 8.   Infiltration capacity based on variations in soil geophysical constants, k

The f value in the curve depicted in Figure 8 signifies the infiltration capacity determined using Equation 2. The soil geophysical constant value, k, is determined using Equation 8 and categorized based on the geophysical constant interval derived from field observations. The calculations for low soil geophysical constant values in the $1.2 < k \leq 1.9$ range, derived from 39 observations, yielded an average infiltration capacity of 625.1 mm/hour. For the interval of values $1.9 < k \leq 2.6$, an

infiltration capacity of 587.7 mm/hour was derived from 31 measurements. In the case of elevated soil geophysical constant values within the range of 2.6<k≤3,3, 30 observations yielded an average infiltration capacity of 499 mm/hour.

The curve results show that the geophysical constant value of small soil results a low infiltration capacity value, and the geophysical constant value of large soil causes a high infiltration capacity. This is because geophysical constants are related to hydraulic conductivity (soil permeability), directly affecting soil infiltration capacity. Soils with high hydraulic conductivity have larger and more pores so that more water can be absorbed more quickly into the soil. This means that the infiltration capacity has increased. In contrast, soils with low hydraulic conductivity have smaller and fewer pores, so water seeps into the soil slower and less. This leads to decreased infiltration capacity, making the soil more susceptible to waterlogging at the surface.

4. Conclusion

The soil characteristics of Padang residential land consist of the soil texture of sand, loamy sand, and sandy loam. High moisture content, large soil content weight, and low porosity cause the soil to become compact and inhibit the infiltration rate. As a result, water is difficult to seep into the soil, especially in the upper layers, which contributes to producing high surface flow. The results of infiltration measurements without artificial infiltration show a constant infiltration rate that falls into the medium category but remains low based on the classification of the catch-land. This low infiltration is caused by high soil density, low porosity, and physical properties of the soil that are not accountable for infiltration. Artificial infiltration proves to be effective in addressing these conditions, significantly increasing the infiltration rate and allowing the soil to absorb water faster and in larger amounts.

The soil infiltration capacity decreases as the soil geophysical constant, k, increases. In soil with a low geophysical constant (k<1.9), the average infiltration capacity attains 625.1 mm/hour. In soil with a high geophysical constant (k>2.6), the average infiltration capacity decreases to 499 mm/hour. Therefore, soil texture and geophysical constants significantly influence infiltration capacity. Sandy soil has the greatest infiltration capability due to its substantial particle size and ample pore space. The soil geophysical constant, associated with hydraulic conductivity, influences infiltration capacity. Soils exhibiting high hydraulic conductivity have superior infiltration capacity, whereas low conductivity results in diminished infiltration capacity, hence improving the danger of waterlogging.

Author's declaration

Author contribution

Totoh Andayono: Conceptualization, Methodology, Investigation, Writing - Original Draft and Writing - Review & Editing. **Mas Mera:** Conceptualization, Supervision and Writing - Review & Editing. **Junaidi**: Software, Validation and Data Curation. **Dalrino**: Software, Validation and Data Curation.

Funding statement

Acknowledgements

Competing interest

The authors declare that they have no known competing financial interests or personal relationships that could have appeared to influence the work reported in this paper.

Ethical clearance

This research does not involve humans or animals as subjects.

AI statement

The Grammarly was used to check the language structure and use of this article. However, the results have been reviewed and verified by an English language expert, thus the authors are fully responsible for the publication content.

Publisher's and Journal's note

Universitas Negeri Padang as the publisher and the editor of Teknomekanik state that there is no conflict of interest towards this article publication.

References

[1] I. G. Dwinanda, K. A. C. Adelia, R. W. Wilda, F. Afli, T. P. Kaloka, and D. L. Pratiwie, "Predictive Mapping of Hydrometeorological Disaster Prone Areas in Central Kalimantan," *Jurnal Penelitian Pendidikan IPA*, vol. 10, no. 2, pp. 811–819, Feb. 2024, https://doi.org/10.29303/jppipa.v10i2.6238

[2] R. Ramadhan *et al.*, "Trends in rainfall and hydrometeorological disasters in new capital city of Indonesia from long-term satellite-based precipitation products," *Remote Sens Appl*, vol. 28, p. 100827, Nov. 2022, https://doi.org/10.1016/j.rsase.2022.100827

[3] P. Syldon, B. B. Shrestha, M. Miyamoto, K. Tamakawa, and S. Nakamura, "Assessing the impact of climate change on flood inundation and agriculture in the Himalayan Mountainous Region of Bhutan," *J Hydrol Reg Stud*, vol. 52, Apr. 2024, https://doi.org/10.1016/j.ejrh.2024.101687

[4] Z. W. Kundzewicz *et al.*, "Le risque d'inondation et les perspectives de changement climatique mondial et régional," *Hydrological Sciences Journal*, vol. 59, no. 1, pp. 1–28, 2014, https://doi.org/10.1080/02626667.2013.857411

[5] David. Fisher, Kirsten. Hagon, Charlotte. Lattimer, Sorcha. O'Callaghan, Sophia. Swithern, and Lisa. Walmsley, *World disasters report 2018 : leaving no one behind*. International Federation of Red Cross and Red Crescent Societies is, 2018. https://www.ifrc.org/document/world-disasters-report-2018

[6] L. Gao, L. Zhang, Y. Hong, H.-X. Chen, and S.-J. Feng, "Flood hazards in urban environment," *Georisk: Assessment and Management of Risk for Engineered Systems and Geohazards*, pp. 1–21, Apr. 2023, https://doi.org/10.1080/17499518.2023.2201266

[7] H. Marhaento, M. J. Booij, and A. Y. Hoekstra, "Hydrological response to future land-use change and climate change in a tropical catchment," *Hydrological Sciences Journal*, vol. 63, no. 9, pp. 1368–1385, Jul. 2018, https://doi.org/10.1080/02626667.2018.1511054

[8]   B. Surya, A. Salim, H. Hernita, S. Suriani, F. Menne, and E. S. Rasyidi, "Land use change, urban agglomeration, and urban sprawl: A sustainable development perspective of makassar city, indonesia," *Land (Basel)*, vol. 10, no. 6, 2021, https://doi.org/10.3390/land10060556

[9]   R. Har, Aprisal, W. D. Taifur, and T. H. A. Putra, "The effect of land uses to change on infiltration capacity and surface runoff at latung sub watershed, Padang City Indonesia," in *E3S Web of Conferences*, EDP Sciences, Dec. 2021. https://doi.org/10.1051/e3sconf/202133108002

[10]   F. Cleophas *et al.*, "Effect of soil physical properties on soil infiltration rates," in *Journal of Physics: Conference Series*, Institute of Physics, 2022. https://doi.org/10.1088/1742-6596/2314/1/012020

[11]   S. Bahddou, W. Otten, W. R. Whalley, H. C. Shin, M. El Gharous, and R. J. Rickson, "Changes in soil surface properties under simulated rainfall and the effect of surface roughness on runoff, infiltration and soil loss," *Geoderma*, vol. 431, Mar. 2023, https://doi.org/10.1016/j.geoderma.2023.116341

[12]   M. Yu, S. Mapuskar, E. Lavonen, A. Oskarsson, P. McCleaf, and J. Lundqvist, "Artificial infiltration in drinking water production: Addressing chemical hazards using effect-based methods," *Water Res*, vol. 221, p. 118776, Aug. 2022, https://doi.org/10.1016/j.watres.2022.118776

[13]   M. Abu-Zreig, H. Fujimaki, and M. A. A. Elbasit, "Enhancing water infiltration through heavy soils with sand-ditch technique," *Water (Switzerland)*, vol. 12, no. 5, May 2020, https://doi.org/10.3390/W12051312

[14]   X. Qing *et al.*, "Research Progress of Soil Water Infiltration," in *E3S Web of Conferences*, EDP Sciences, Sep. 2020. https://doi.org/10.1051/e3sconf/202018901006

[15]   Z. Boukalová, J. Těšitel, Z. Hrkal, and D. Kahuda, "Artificial infiltration as an integrated water resources management tool," *WIT Transactions on Ecology and the Environment*, vol. 182, no. October, pp. 201–210, 2014, https://doi.org/10.2495/WP140181

[16]   S. M. Ghabayen, A. Nassar, S. El Dirawi, H. Rashwan, and H. Sarsour, "Enhancement of Artificial Infiltration Capacity in Low Permeability Soils for Gaza Coastal Aquifer," *Environment and Natural Resources Research*, vol. 3, no. 4, pp. 155–166, 2013, https://doi.org/10.5539/enrr.v3n4p155

[17]   LHCCREM, "Infiltration Devices." [Online]. Available: https://www.newcastle.nsw.gov.au/Newcastle/media/Documents/environment

[18]   X. Meng *et al.*, "Improved stormwater management through the combination of the conventional water sensitive urban design and stormwater pipeline network," *Process Safety and Environmental Protection*, vol. 159, pp. 1164–1173, Mar. 2022, https://doi.org/10.1016/j.psep.2022.02.003

[19]   W. Wu, B. Jamali, K. Zhang, L. Marshall, and A. Deletic, "Water Sensitive Urban Design (WSUD) Spatial Prioritisation through Global Sensitivity Analysis for Effective Urban Pluvial Flood Mitigation," *Water Res*, vol. 235, p. 119888, May 2023, https://doi.org/10.1016/j.watres.2023.119888

[20]   A. A. Jennings and K. Baker, "Hydraulic Performance of a Residential Stormwater Infiltration Gallery," *Journal of Environmental Engineering (United States)*, vol. 142, no. 3, pp. 1–9, 2016, https://doi.org/10.1061/(ASCE)EE.1943-7870.0001063

[21]   V. Kirenda and S. N. Mugume, "Effectiveness of infiltration galleries in reduction of surface runoff and flooding in urban areas," *Conference: Novatech 2019 At: Lyon,* July, pp. 1–6, 2019.

[22]   M. Fahim Aslam, M. Habib-ur-Rehman, and N. Muhammad Khan, "Assessing the Role of Infiltration Galleries to Enhance Groundwater Recharge in Model Town Lahore," *American Journal of Water Science and Engineering*, vol. 7, no. 1, p. 14, 2021, https://doi.org/10.11648/j.ajwse.20210701.12

[23]   J. C. Y. Guo, "Drain Time for Porous Stormwater Basin," *J Hydrol Eng*, vol. 25, no. 5, p. 04020017, 2020, https://doi.org/10.1061/(asce)he.1943-5584.0001915

[24] Y. Liu, Z. Cui, Z. Huang, M. López-Vicente, and G. L. Wu, "Influence of soil moisture and plant roots on the soil infiltration capacity at different stages in arid grasslands of China," *Catena (Amst)*, vol. 182, Nov. 2019, https://doi.org/10.1016/j.catena.2019.104147

[25] M. Hidayat, D. Djufri, H. Basri, N. Ismail, R. Idroes, and M. F. Ikhwali, "Influence of vegetation type on infiltration rate and capacity at Ie jue geothermal manifestation, Mount Seulawah Agam, Indonesia," *Heliyon*, vol. 10, no. 4, Feb. 2024, https://doi.org/10.1016/j.heliyon.2024.e25783

[26] U. Fitriati and K. Malikur Rahman, "Relationship Between Soil Physical Characteristics and Infiltration Rate of The Practice Area of SMK PPN Banjarbaru," *Civil and Environmental Science*, vol. 6, no. 2, pp. 117–123, Oct. 2023, https://doi.org/10.21776/civense.v6i2.408

[27] W. Lei, H. Dong, P. Chen, H. Lv, L. Fan, and G. Mei, "Study on Runoff and Infiltration for Expansive Soil Slopes in Simulated Rainfall," *Water (Switzerland)*, vol. 12, no. 1, Jan. 2020, https://doi.org/10.3390/w12010222

[28] J. R. Philip, "Theory of Infiltration," in *Advances in Hydroscience*, vol. 5, Academic Press, INC., 1969, pp. 215–296. https://doi.org/10.1016/b978-1-4831-9936-8.50010-6

[29] ASCE, "Chapter 3 : Infiltration," in *Hydrology Handbook*, vol. 0, G. D. of the A. S. of C. Engineers, Ed., American Society of Civil Engineers (ASCE), 1996, pp. 75–124. http://ndl.ethernet.edu.et/bitstream/123456789/61345/1/1098.pdf

[30] H. Rusli, S. Hasibuan, D. A. Tanjung, M. Saragih, R. Setia Budi, and M. Paramuji, "Investigation of Water Content, Soil Density, Hydraulic Conductivity and Matrix Suction on Infiltration Rate in Padang City-Indonesia," vol. 8, no. 2, pp. 156–163, 2024, https://doi.org/10.26480/wcm.02.2024.156.163

[31] T. Andayono, M. Mera, Junaidi, Dalrino, R. Maiyudi, and A. H. Burhamidar, "Artificial Infiltration Model to Increase Infiltration Capacity in Urban Residential land," *Water Conservation and Management*, vol. 8, no. 4, pp. 396–401, 2024, https://doi.org/10.26480/wcm.04.2024.396.401

[32] Eijkelkamp, "Double Ring Infiltrometer Manual," *Double Ring Infiltrometer*, pp. 1–9, 2015. https://soilmoisture.com/wp-content/uploads/2024/07/Resource_Instructions_0898-2830_2830K1-Double-Ring-Infiltrometer.pdf

[33] Badan Standardisasi Nasional, "*SNI 7752:2012: Tata cara pengukuran laju infiltrasi di lapangan menggunakan infiltrometer cincin ganda dengan cincin dalam tertutup [SNI 7752:2012: Procedure for measuring infiltration rate in the field using a double-ring infiltrometer with a closed inner ring]*". Jakarta : Badan Standardisasi Nasional. 2012